https://doi.org/10.5194/wes-2022-14
Preprint. Discussion started: 22 March 2022

eawe european academy of wind energy
Open Access WIND ENERGY SCIENCE DISCUSSIONS

Optimization of wind farm portfolio to minimize the overall power fluctuations - a case study for the Faroe Islands

Turið Poulsen[1], Bárður A. Niclasen[1], Gregor Giebel[2], and Hans Georg Beyer[1]

[1]Faculty of Science and Technology, University of the Faroe Islands
[2]Department of Wind Energy, Technical University of Denmark

Correspondence: Turið Poulsen (turidp@setur.fo)

Abstract. Hourly modeled wind turbine power output time series - modeled from outputs from the mesoscale numerical weather prediction system WRF - are used to examine the spatial smoothing of various wind farm portfolios located on a complex isolated island group with a surface area of 1400 km^2. Power spectral densities (PSD), hourly step change functions, and duration curves are generated, and the 5th and 95th percentiles of the step change functions are calculated. The spatial smoothing is identified from smaller high frequency PSD values, less hourly fluctuations, and more flat duration curves per installed wind power capacity, compared to single wind turbine outputs. A discussion on the limitation of the spatial smoothing for the region is included, where a smoothing effect is clear for periods up to 1-2 days, although most evident at the higher frequencies. By maximizing the smoothing effect, optimal wind farm portfolios are presented with the intention to minimize the overall wind power fluctuations. The focus is mainly on the smoothing effect in highest resolvable frequencies. Optimizing wind farm capacities at fourteen pre-defined good wind farm site locations has a minimal improvement on the hourly fluctuations. However, choosing good combinations of the individual wind farm site locations decrease the 1-3 hourly fluctuations considerably; the optimized wind farm portfolios consist of distant wind farms, while poor portfolios consist of clustered wind farms. The 5th and 95th percentiles are 15% less for an optimized portfolio with four wind farms compared to a poor combination of four wind farms.

1 Introduction

Most nations are striving to make their electricity generation less dependent on fossil fuels. Wind power is an attractive solution, being environmentally friendly, mature, and affordable. Integrating a large fraction of wind power into a power grid system can create challenges, as wind varies at various time scales. Measures are required to mitigate the natural wind power fluctuations in order to balance and keep the grid stabilized. One possible measure is spatial distribution of wind farm siting, see e.g. Beyer et al. (1990) or Katzenstein et al. (2010). Isolated grids have special challenges, as they usually span over small areas, and the available wind resource is thus partly or fully co-varying, inflicting a serious challenge for maintaining energy balance on the grid.

This study examines the wind power fluctuations for different wind farm portfolios in a confined isolated region. The goal is to analyze and optimize the smoothing effect caused by the nature of dispersed wind farm sites, where the Faroe Islands is used

https://doi.org/10.5194/wes-2022-14
Preprint. Discussion started: 22 March 2022

Figure 1. A map generated with the software © Google Earth Pro (see affiliation on the map). The red circle marks the position of the Faroe Islands.

as a case study. The Faroe Islands is a small isolated mountainous islands group (1400 km^2) in the north-east of the Atlantic Ocean, ∼300 km apart from other main-lands, see Fig. 1. The topography is complex and the climate is windy.

Hourly modeled wind turbine power output data are used to generate power spectral densities (PSD), hourly step change functions, and duration curves for individual and lumped power output time series. Moreover, the 5th and 95th percentiles of the step change functions are extracted as a measure to quantitatively compare results. Optimizations of wind farm siting on the Faroe Islands are carried out with the objective to minimize the high frequency power output fluctuations of the lumped time series.

There exist numerous studies in the literature analyzing the smoothing effect of spatial distributed wind farm sites at various time and spatial scales, applying different techniques, e.g. correlation analyzes (Beyer et al., 1993; Katzenstein et al., 2010; Pearre and Swan, 2018; Giebel, 2000), step change analysis (Beyer et al., 1990, 1993; Katzenstein et al., 2010; Pearre and Swan, 2018; Giebel, 2000), visualization of duration curves (Giebel, 2000; Barasa and Aganda, 2016; Katzenstein et al., 2010), and analysis in the frequency domain (Beyer et al., 1990, 1993; Nanahara et al., 2004b, a; Katzenstein et al., 2010; Poulsen and Beyer, 2020). One advantage with frequency analysis is the ability to characterize the extend of the smoothing effect for many frequencies. The reduction of the total variance of aggregated wind farm data can be small even though a significant smoothing effect occurs at higher frequencies, as observed by Beyer et al. (1990). On the other hand, time domain analysis - such as step change analysis and duration curves - may be more intuitive to interpret. Other examples of studies analyzing the smoothing of spatial distributed wind farms in the time domain include Palutikof et al. (1990), Wan et al. (2003), and Giebel (2001).

Frank et al. (2021) is an example of a resent study examining the smoothing effect of the natural variability of both wind and solar power. They analyzed daily data from eleven European countries. Although their focus was both on wind and solar power, the smoothing effect from spatial distributed wind power is seen within their results, from low correlation coefficients and low joint probabilities of minimum and maximum wind power between the countries. In addition, they optimize the installation

https://doi.org/10.5194/wes-2022-14
Preprint. Discussion started: 22 March 2022

eawe european academy of wind energy
Open Access WIND ENERGY SCIENCE DISCUSSIONS

ratio between solar and wind power, in order to reduce the extreme fluctuations. Even though their results can not be directly compared to results in this study, their study demonstrates the potential of balancing natural fluctuations from renewable energy resources by considering the configuration of the resources.

Reichenberg et al. (2014) and Cassola et al. (2008) are examples of studies focusing on minimizing the fluctuation of the total wind power production through wind farm optimization. Reichenberg et al. (2014) develop a method, optimizing the location of wind farms, by minimizing the coefficient of variation of the total wind power output time series. Their method is based on the sequential optimization of the selection of wind farm site locations, and it is applied to the Nordic countries and Germany. Cassola et al. (2008) propose a procedure to optimally distribute the relative size of considered wind farms, by minimizing either the variation of the total wind power output time series, or by minimizing the ratio between the variation and the total wind energy production. Their method was tested for wind power data at ten locations in Corsica (France), a complex island in the Mediterranean Basin, stretching 175 km in the latitude direction and 80 km in the longitude direction, with a mountain chain crossing the islands in the north-south direction with peaks higher than 2000 m. The results from these studies can nor be directly compared to the results obtained in this study, as the methodologies are different, as well as the geographic.

The methodology applied in the presented wind farm portfolio optimization study is unconventional, using spectral results as the objective function to minimize the overall wind power fluctuations, being a powerful methodology in the sense that the optimization focuses solely on the preferred frequencies. Furthermore, no such optimization study has ever been conducted for the Faroe Islands region.

The data sets used in this study are introduced in Sect. 2. The methods applied are described in Sect. 3. The results are presented in Sect. 4. And a summary and conclusions are given in Sect. 5.

2 Data

Hourly WRF-generated wind speed data is the primary data set used throughout the study. Time series are extracted at locations with favourable wind farm conditions. In addition, available empirical data are used for comparison.

2.1 WRF-generated wind speed data

WRF-generated data are simulated by Kjeller Vindteknikk and made available to us via SEV (the local power company of the Faroe Islands). The model setup is documented in Haslerud (2019). Multiple output parameters were generated, including wind speed data used in this study, validated by Poulsen et al. (2021). WRF version v3.8.1 was used for the simulations, with 51 vertical levels (8 in the lower 200 m). Three nested domains were used, with horizontal resolutions of 500m x 500m, 1500m x 1500m, and 7500m x 7500m, for the innermost, middle, and outer domain, respectively. The innermost domain covered the entire Faroe Islands. Data was stored every hour during the period 1. July 2016 to 30. June 2018. The Thompson scheme, the Mellor-Yamada-Janjik scheme, and the NOAH scheme were applied for the microphysics, the boundary layer mixing, and the surface, respectively. Every 3 hours, ERA5 reanalysis data with a horizontal resolution of approximately 0.25 degrees was used as boundary conditions (available from the European Centre for Medium-Range Weather Forecasts, ECMWF).

https://doi.org/10.5194/wes-2022-14
Preprint. Discussion started: 22 March 2022

eawe european academy of wind energy
Open Access WIND ENERGY SCIENCE DISCUSSIONS

2.2 Empirical data

During the period 1. July 2016 to 30. June 2018, hourly power production data from three wind farms operating on the Faroe Islands are available. The hub heights of all turbines (except one smaller) are 45 m a.g.l. In addition, 10 min averaged wind speed measurements from an additional site at a height of 52.8 m a.g.l. during the period 21. July 2016 to 30. June 2018 are available. The location of the four sites are pinpointed in Fig. 2.

2.3 Favourable wind farm site locations

Magnussen (2017) presents a map with current and potential wind farm siting areas on the Faroe Islands, see Fig. 2. The areas were selected based on modeled wind resource, distance from road, distance from high voltage grid, terrain slope, populated area, waters and rivers. These considerations were weighted and merged. Based on additional considerations, as e.g. expected turbulent areas, further locations were rejected, and the selection of favorable wind farm sites was composed.

Data at these favourable locations are used throughout the study.

3 Method

Modeled wind turbine power output data at a height of 45 m a.g.l are examined during the period July 2016 to June 2018. The data process of the time series is explained in the following subsection. The applied analytical methods are defined in the second subsection, while the final subsection discusses the ignored smoothing effect within wind farms.

3.1 Data processing

WRF-generated wind speed time series for selected sites are vertically interpolated to a height of 45 m a.g.l. These time series are then corrected for aliasing effect, as elaborated on in the appendix.

The wind speed time series are modeled to power output time series using a power curve of an Enercon E-44 wind turbine with storm control function (Enercon, 2012).

To be able to compare results, all power output time series are normalized by their rated wind power capacity. When time series are aggregated, the lumped time series is computed prior to the normalization.

3.2 Approaches for the characterization of the power output time series

The study applies three analysing techniques to the time series - spectral analysis, step change analysis, and the generation of duration curves - each elaborated on in the following subsections. The former two characterize the time series fluctuations, while the latter characterizes the distribution of the power generation.

https://doi.org/10.5194/wes-2022-14
Preprint. Discussion started: 22 March 2022

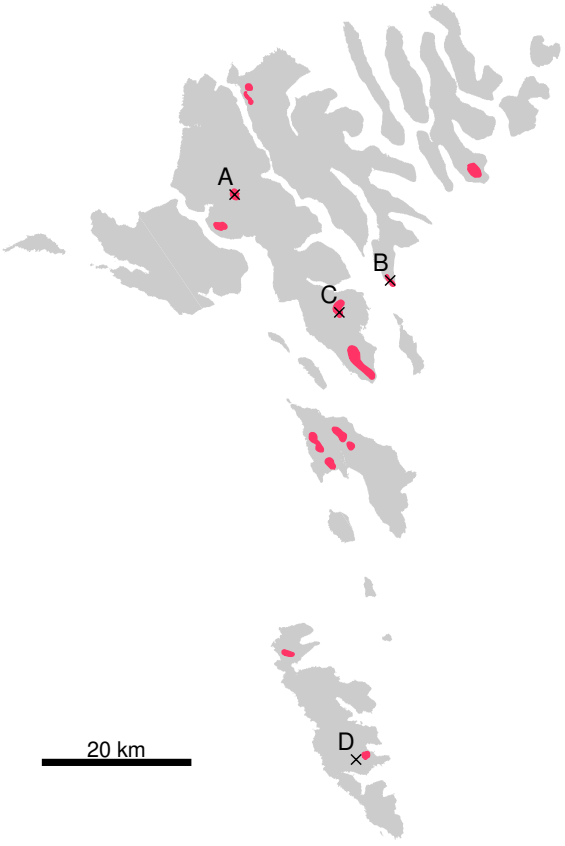

Figure 2. Gray areas mark the terrain of the Faroe Islands. Red patches mark current and potential wind farm locations as selected by Magnussen (2017). Black markers pinpoint sites where actual measured data are available during the period June 2016 to July 2018, denoted with the letters A to D. The area of the terrain are created using 10 m raster map extracted from https://www.foroyakort.fo/ 18. Dec. 2020, created in Denmark from satellite data 2017.

3.2.1 Spectral analysis

PSD are generated for normalized power output time series using Fourier transform. Only the values corresponding to the positive frequencies of the Fourier transform are extracted. Thus, the integral of the raw spectra with respect to frequency yields about half of the variance of the time series. Due to the inherent uncertainty of the raw spectral estimates, smoothed PSD are generated by dividing the time series up in chunks, calculating the spectral results for each chunk, then average over all chunks. For each chunk, the average value is subtracted and a hamming window is applied. A 50% overlap between chunks is used.

https://doi.org/10.5194/wes-2022-14
Preprint. Discussion started: 22 March 2022

eawe european academy of wind energy
Open Access WIND ENERGY SCIENCE DISCUSSIONS

3.2.2 Step change analysis

The step change function of the wind power time series is calculated as given in Eq. (1).

$$\Delta P_i = P_{i+1} - P_i \tag{1}$$

where P_i is the wind power production at time i, P_{i+1} is the wind power production at the consecutive time stamp, and ΔP_i is the corresponding change in the wind power production between these two time stamps. The distribution of the wind power step change function is presented with its probability density function (pdf). In addition, the 5th and 95th percentiles of the step change function are identified.

3.2.3 Extraction of power duration curves

The data from the power output time series are sorted according to descending magnitude to extract the fraction of exceedance of power levels, presenting the power duration curve.

3.3 A note on ignoring the wind farm smoothing effect

This study analyzes turbine outputs, thus neglects potential smoothing effect within wind farms. Various studies investigate the coherence function between time series at a wind farm scale (Schlez and Infield, 1998; Vigueras-Rodríguez et al., 2012; Vincent et al., 2013); the coherence function can be used as a measure of the smoothing effect between time series as a function of frequency. If the coherence is high, the smoothing effect is small at the considered frequency range. If the coherence is small, a smoothing effect occurs.

The distance between the two farthest turbines in the currently largest wind farm in the Faroe Islands - with thirteen 0.9 MW turbines - is about 670 m. For a wind speed of 10 m/s (approximate average values as observed for the Faroe Islands region by Poulsen et al. (2021)), a distance of 670 m, and a frequency of $2^{-1}\mathrm{h}^{-1}$, the analytical coherence model presented by Vigueras-Rodríguez et al. (2012) yields squared coherence values of 0.81 and 0.92 for lateral and longitudinal directions, respectively, and the wind farm smoothing effect is therefore expected to be small for frequencies up to $2^{-1}\mathrm{h}^{-1}$. For larger wind farms, a wind farm smoothing effect could be expected. Although, outside the scope of this study, a more detailed study could apply methods such as those presented by Nørgaard and Holttinen (2004) or Sørensen et al. (2008) when scaling up turbine outputs to large wind farms.

4 Results

All results represent normalized power output time series with respect to its total rated power. This enables comparisons between results.

First, statistical characteristics of modeled turbine power output time series from WRF-generated wind speeds are compared to those of measured data. In the subsequent subsection, the modeled turbine power output time series are used to optimize

https://doi.org/10.5194/wes-2022-14
Preprint. Discussion started: 22 March 2022

eawe european academy of wind energy
Open Access WIND ENERGY SCIENCE DISCUSSIONS

Table 1. 5th and 95th percentiles of the hourly step change function of power outputs modeled from WRF-generated wind speeds (P_{WRF}) and empirical data (P_{Emp}) (see Fig. 2 for site locations). The lumped time series assumes an equal distribution of wind power capacity at all four locations. All time series are normalized by their rated power.

		site A	site B	site C	site D	Lumped time series
P_{WRF}	5th percentile	-0.200	-0.200	-0.183	-0.172	-0.113
	95th percentile	0.202	0.201	0.174	0.170	0.117
P_{Emp}	5th percentile	-0.194	-0.190	-0.156	-0.180	-0.110
	95th percentile	0.199	0.188	0.153	0.180	0.114

wind farm capacities at selective wind farm site locations, with the objective to minimize the high frequency fluctuations of the aggregated time series. Limitations on the spatial wind farm smoothing effect in the small islands system are discussed in the third subsection. Finally, optimization of the geographical distribution of wind farms are presented in the fourth subsection.

4.1 Comparing statistical characteristics of WRF modeled and measured data set

To examine the validity of the modeled turbine power output data from WRF-generated wind speeds, these time series are compared to actual measurements. Three wind farms were operating on the Faroe Islands during the period July 2016 to June 2018, the period of the WRF-generated data. One additional measured time series is gained by converting meteorological data to turbine output data.

PSD, pdf of hourly step change functions, and duration curves for site specific and lumped wind farm power output data are calculated and depicted in Fig. 3; the lumped time series equally weights the installed capacity at the four site locations. The site specific PSD and pdf display similar behaviours as observed for measurements. However, the PSD values at the highest frequencies are somewhat overestimated at sites B and C. This is also clear from the 5th and 95th percentiles presented in Table 1. The duration curves have evident site specific deviations.

4.2 Optimization of wind farm capacities

By optimizing the wind power capacity of scattered wind farms with the aim to minimize the fluctuations of the total time series, the most stable wind farm configuration is derived. For this purpose, modeled wind turbine output data at predefined locations are used - the favourable wind farm locations in the region as selected by Magnussen (2017), see Sect. 2.3. The focus of the optimization is the fluctuations at the highest resolvable frequencies.

The optimization is carried out using the gradient based interior-point optimization algorithm. The objective function is set to be the integrated PSD values of the total wind power time series for frequencies between $3^{-1}\mathrm{h}^{-1}$ and $2^{-1}\mathrm{h}^{-1}$:

https://doi.org/10.5194/wes-2022-14
Preprint. Discussion started: 22 March 2022

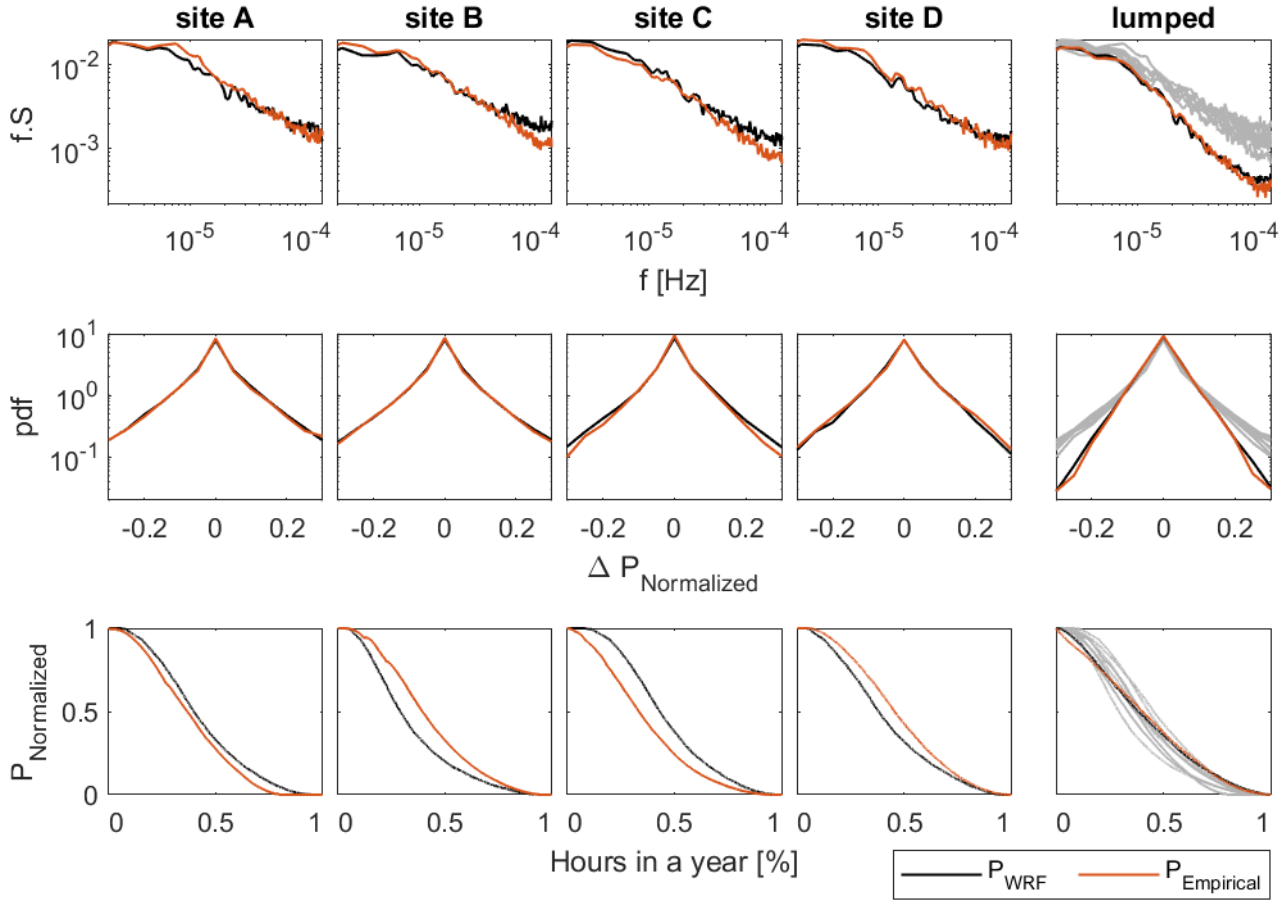

Figure 3. PSD (top), pdf of hourly step change functions (middle), and duration curves (bottom) per rated wind power capacity. Black colors represent results developed from WRF-generated data. Red colors represent results developed from measured data. First four columns represent data from individual sites. The last column represent the lumped time series of all four sites, with an equal distribution of wind power capacity at all four locations.

$$\text{minimize:} \quad \int_{(3\text{h})^{-1}}^{(2\text{h})^{-1}} \text{PSD}\, df \tag{2}$$

thus, minimizing the two-three hourly fluctuations of the lumped time series. The optimized parameters are the capacities of the individual wind farms normalized by the total installed capacity. Thus, one constrain of the optimization algorithm is that the sum of the optimized parameters equals one:

https://doi.org/10.5194/wes-2022-14
Preprint. Discussion started: 22 March 2022

eawe european academy of wind energy
Open Access WIND ENERGY SCIENCE DISCUSSIONS

$$\sum_{i=1}^{n} P_{max,i} = 1 \tag{3}$$

where $P_{max,i}$ is the wind farm capacity at site location i, and n is the total number of considered wind farm site locations. A wind farm capacity is always greater or equal to zero:

$$\forall i \leq n, \qquad P_{max,i} \geq 0 \tag{4}$$

The optimization algorithm is conducted for three cases:

Case I: Considering all fourteen favourable wind farm site locations mapped in Fig. 2.

Case II: Excluding the two southernmost wind farm site locations.

Case III: Upper and lower boundaries for the installed wind power capacity are given to each of the fourteen wind farms.[1]

The optimized wind farm configurations for the three cases are presented in Fig. 4. The distributions of the optimized wind farm capacities are logical, with generally more capacities at more remote sites and less capacities for closely clustered wind farm sites. However, the effect of the optimization is limited compared to if the wind power capacity were to be equally distributed over all considered sites. The reduction of the 5th and 95th percentiles of the hourly step change functions is 2% or less for the three optimized cases.

PSD, pdf of the hourly step change functions, and the duration curves of the optimized lumped time series are displayed in Fig. 5. For reference, results from single turbine outputs are superimposed. The 5th and the 95th percentiles of the step change functions are given in Table 2.

No clear distinction can be observed in pdf of the step change functions and the duration curves for the three cases. However, a smoothing effect is observed compared to the single turbine outputs, with lower hourly step changes, and less frequent intervals with zero and rated power production.

The spectra for all the cases are equivalent for low frequencies and similar to those of the single turbine outputs, while the energy content in the higher frequencies differ. A smoothing effect for the combined time series (cases I-III) compared to the single turbine outputs is most evident at the highest frequencies, but clear for periods up to 1-2 days.

Out of the three cases, case II (the exclusion of the two southernmost site locations) has the heaviest spectral tail, followed by Case III (bound by current and committed wind farm power capacities) and finally case I (all site locations). The 5th and 95th percentiles of the hourly step change functions of the time series show the same trend, with highest values for case II, followed by case III, then case I. Excluding the two southernmost site locations increases the 5th and 95th percentiles by 7%, while setting boundaries to the lower and upper wind farm capacities increases the percentiles with 3%.

[1]Upper bounds are defined from the site specific area marked in Magnussen (2017). For each 30000 m^2 ($3 \cdot 44$ m $\cdot 5 \cdot 44$ m $\sim$30000 m^2), 0.9 MW is added to the possible upper boundary - The rotor diameter of an Enercon E44 turbine is 44 m, currently the most frequent turbine model on the Faroe Islands. However, none of the optimized values exceed the upper boundaries, making the upper boundaries redundant. The lower boundaries are set to be the capacity of the current and committed wind farms on the Faroe Islands as distributed in the study by Tróndheim et al. (2021), in total 60.63 MW. Values for both upper and lower boundaries are normalized by a total power capacity of 168 MW, being the proposed wind power capacity in 2030 by Tróndheim et al. (2021).

https://doi.org/10.5194/wes-2022-14
Preprint. Discussion started: 22 March 2022

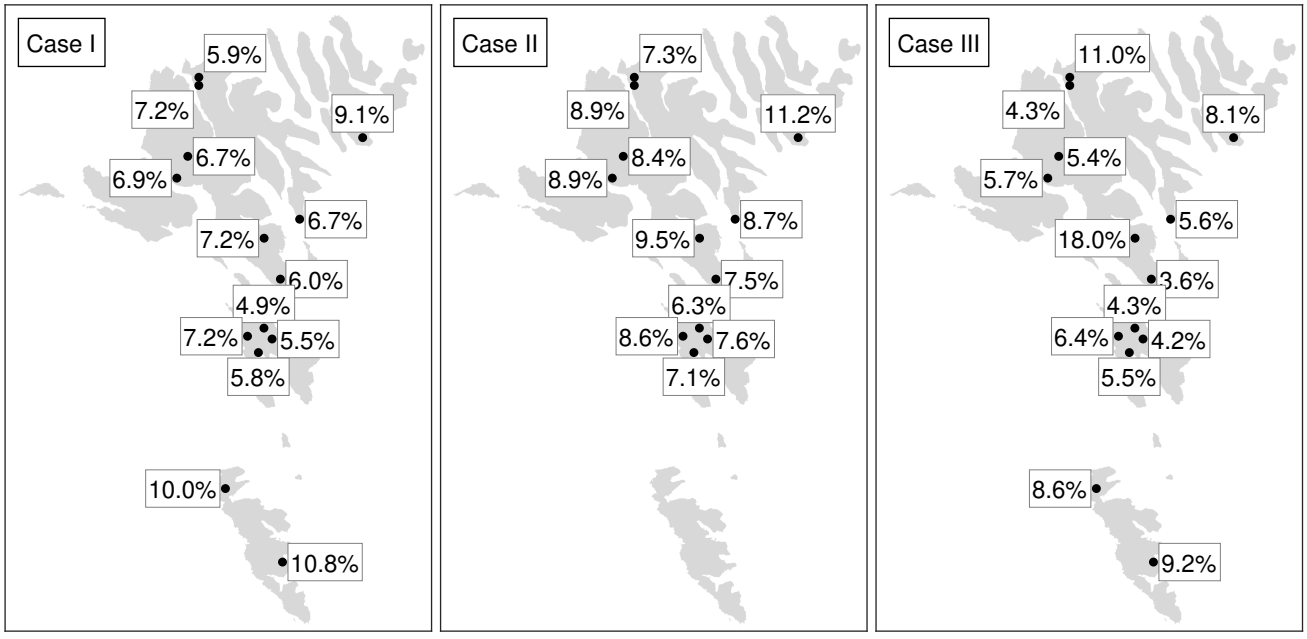

Figure 4. Optimized wind farm configurations, shown in percentages of site specific wind power capacity per total installed wind power capacity. Case I: Considering all fourteen favourable wind farm locations selected by Magnussen (2017). Case II: excluding the two southernmost sites. Case III: setting site specific lower and upper boundaries for the wind farm capacities at the fourteen sites. The area of the terrain are created using 10 m raster map extracted from https://www.foroyakort.fo/ 18. Dec. 2020, created in Denmark from satellite data 2017.

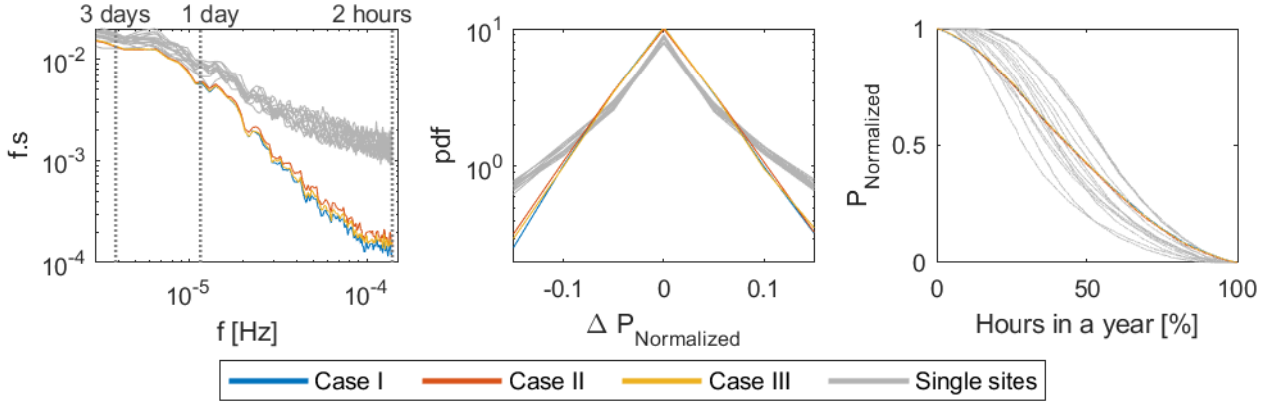

Figure 5. PSD (left), pdf of hourly step change functions (middle), and duration curves (right) of lumped power output time series per installed capacity for the three optimized cases displayed in Fig. 4 and single turbine time series (gray).

https://doi.org/10.5194/wes-2022-14
Preprint. Discussion started: 22 March 2022

eawe european academy of wind energy
Open Access WIND ENERGY SCIENCE DISCUSSIONS

Table 2. 5th and the 95th percentiles of the hourly step change functions per rated wind power capacity for the three optimized lumped power output time series displayed in Fig. 4.

Percentiles	case I	case II	case III
5th percentiles	-0.0892	-0.0954	-0.0917
95th percentiles	0.0900	0.0964	0.0923

4.2.1 Sensitivity analysis on the PSD of power outputs to the inclusion of remote sites

As observed in Fig. 5 and Table 2, excluding the two time series at the southernmost island increases the optimized lumped time series fluctuation at the highest frequency range considerably. In other words, the inclusion of the two southernmost site locations smooth the total time series.

To test if the smoothing effect originates from the inclusion of two additional sites in the given region, or weather it is because the two sites are further away, PSD for various optimized site combinations are generated and displayed in Fig. 6:

- Including all fourteen sites (case I)
- Excluding the two southernmost sites (case II)
- All possible combinations of twelve sites with the constrain that two out of the twelve sites are those located on the southernmost islands

Case II has higher PSD values at the highest frequency range compared to every other combinations of the twelve site locations that include the two southernmost site locations. Indicating that the smoothing effect at the highest frequencies are more pronounced for remote sites.

4.3 Limitation of spatial distributed wind farms

To test the limitation of the smoothing effect from spatial distributed wind farms in the Faroe Islands, PSD are generated for multiple combination of up to fourteen turbine power output time series; the fourteen favourable site location marked in Fig. 2. Each computation considers an equal distribution of the rated power at all considered sites. Results are displayed in Fig. 7. As the number of lumped time series, n, increases, the PSD values at the highest frequencies decreases. The smoothing effect is evident for periods up to 1-2 days, but more evident for the higher frequencies. The smoothing effect observed when adding one additional wind farm to the lumped time series becomes less pronounce when n is large.

In addition, the PSD of the total power output when combining n wind farms differ in the various combinations of the individual wind farms. This will be analyzed further in the following subsection.

https://doi.org/10.5194/wes-2022-14
Preprint. Discussion started: 22 March 2022

eawe european academy of wind energy
Open Access WIND ENERGY SCIENCE DISCUSSIONS

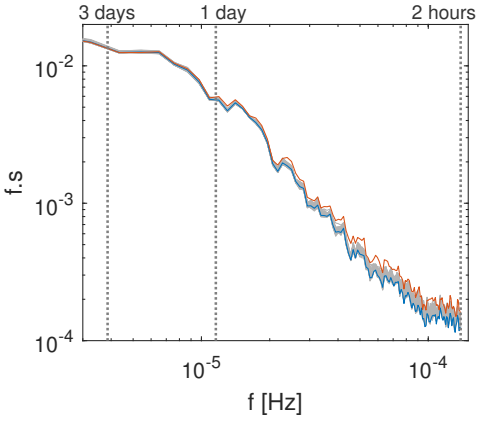

Figure 6. PSD for various optimized combinations of lumped power output time series per installed capacity. Blue line: case I. Red line: case II. Gray lines (sixty-six compressed lines): PSD for all sixty-six possible combinations of twelve lumped power output time series, with the constrain that two of the twelve sites are located on the southernmost islands.

4.4 Optimization of wind farm positioning

As observed from Fig. 7, the same number of lumped wind farm time series can display different PSD, depending on which individual time series are aggregated.

By extracting wind farm combinations with the smallest integrals of the PSD with respect to frequencies from $3^{-1}\mathrm{h}^{-1}$ to $2^{-1}\mathrm{h}^{-1}$, the wind farm combinations with the least fluctuations are obtained. Figures 8 and 9 give examples of good wind farm combinations when $n = 4$ and $n = 7$, respectively. For reference, poor wind farm combinations are also given, those with the highest integrals. It is observed that the wind farms appearing in the favourable combinations, i.e. smallest integrals, are scattered, while the the opposite is observed for the poor combinations.

The 5th and 95th percentiles of the hourly step change function of the lumped time series for each example are also given in Fig. 8 and 9. The percentiles of the favourable combinations are considerably lower compared to the poor combinations, around 15% for $n = 4$ and around 13% for $n = 7$. In addition, the percentiles of the hourly step change function of the lumped time series for all combinations of $n < 14$ wind farms are given in Table 3, together with the corresponding percentiles of the lumped time series with smallest integral.

It can be concluded that the combinations of individual site locations when building n wind farms in the Faroe Islands has a considerable impact on the hourly fluctuations of the total power output time series, information that ought to be of interest to operators. Wind farm portfolio with distant sites are preferred in order to have the most stable lumped wind power time series.

5 Conclusions

The identification of the best distribution of wind farm production within a region is mainly done in terms of identifying the energy yield. But the present study discusses the use of the knowledge on the underling spatial-temporal characteristics of the

https://doi.org/10.5194/wes-2022-14
Preprint. Discussion started: 22 March 2022

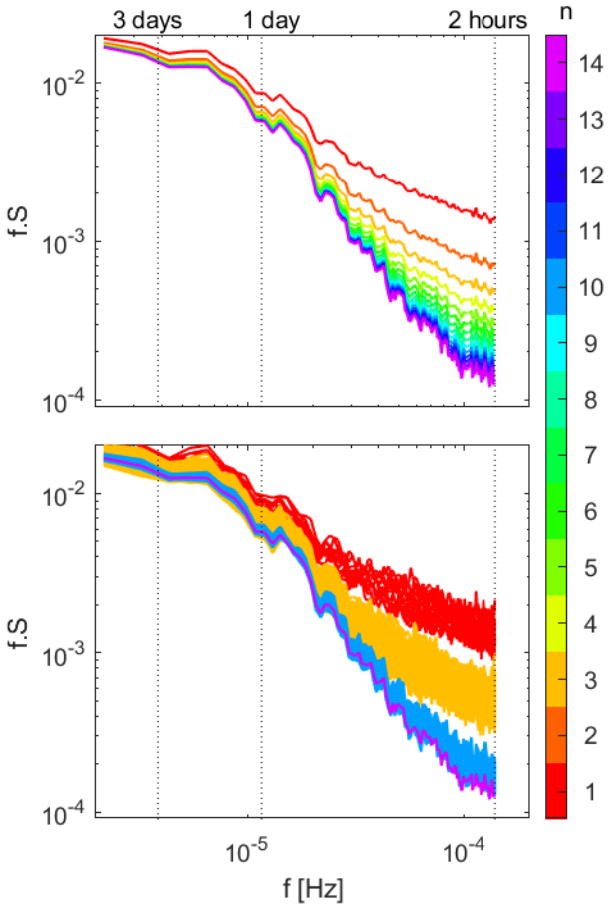

Figure 7. PSD per installed wind power capacity for up to 14 lumped modeled power output time series. All computations consider an equal distribution of the rated power at the considered sites. Colors indicate the number of lumped time series (n). Bottom panel: all possible combinations for n = [1,3,10,14]. Top panel: averaged spectra of all possible combinations for n = [1,2,...,14].

governing wind field to assist in the search on system configurations assuring reduced variability of the power generation. The study investigates the natural smoothing effect from spatial distributed wind farm sites at a small island system with complex terrain, using the Faroe Islands as a case study. For this, hourly modeled wind turbine power output data 45 m a.g.l. are analyzed; converted from WRF-generated wind speed data at fourteen good wind farm site locations as selected by Magnussen (2017). All results are presented per installed wind power capacity, i.e. normalized with respect to the rated power.

The focus is especially on the power output fluctuations at the highest resolvable frequencies, being on hourly scale. PSD, hourly step change functions, and duration curves are generated, and the 5th and 95th percentiles of the hourly step change functions are extracted. As expected from the literature, the smoothing from lumped power output time series is evident, with smaller high frequency PSD values, less hourly fluctuations, and fewer periods with zero and rated power production compared to single wind turbine outputs.

https://doi.org/10.5194/wes-2022-14
Preprint. Discussion started: 22 March 2022

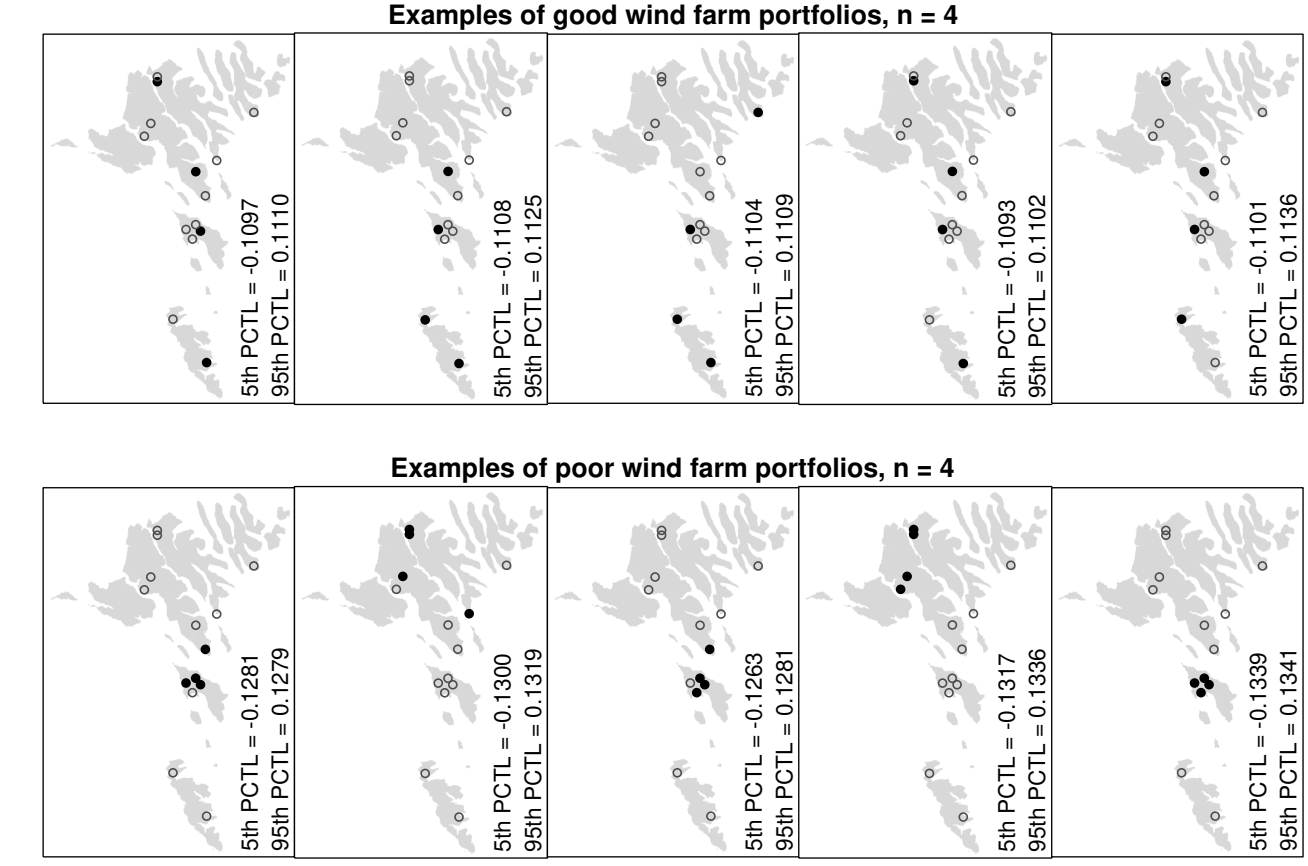

Figure 8. Examples of good (top) and poor (bottom) wind farm portfolios with four wind farms (black filled circles) where the rated power at each wind farm is the same. The open circles mark the other locations that are not selected. Theses examples are the portfolios with the smallest (top) and largest (bottom) integrals of the PSD with respect to frequencies from $3^{-1}\mathrm{h}^{-1}$ to $2^{-1}\mathrm{h}^{-1}$ out of all the possible combinations of four wind farms. The 5th and 95th percentiles (PCTL) of the hourly step change function of the total wind power time series per installed power is given in the bottom right corner of each example.

By strategically distributing wind farms, the spatial smoothing can be maximized, resulting in less regulation effort for the operator. In this study, optimized wind farm portfolios for the Faroe Islands are generated with an objective function set to be the integral of the PSD for frequencies between $3^{-1}\mathrm{h}^{-1}$ and $2^{-1}\mathrm{h}^{-1}$, thus minimizing the 2-3 hourly fluctuations.

245 Wind farm capacities at fourteen pre-defined good wind farm site locations are optimized. The results show that the wind farm capacities at remote sites should be higher, and that the wind farm capacities at clustered sites should be less. However, the optimization has only a small influence on the hourly fluctuations compared to if the wind farm capacities at the pre-defined wind farm site locations were equally distributed over all wind farms. The decrease of the 5th and 95th percentiles of the hourly step change function is about 2%.

https://doi.org/10.5194/wes-2022-14
Preprint. Discussion started: 22 March 2022

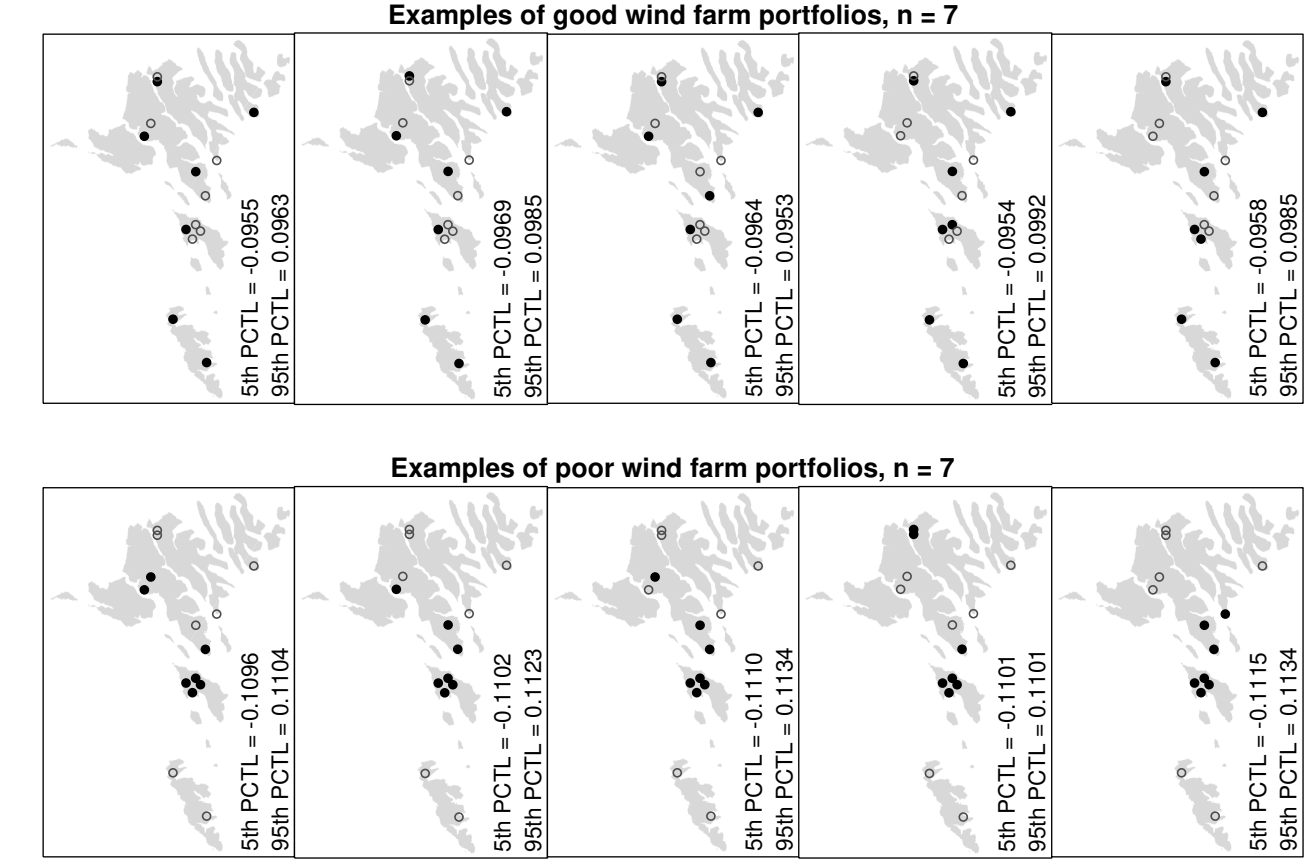

Figure 9. Examples of good (top) and poor (bottom) wind farm portfolios with seven wind farms (black filled circles) where the rated power at each wind farm is the same. The open circles mark the other locations that are not selected. Theses examples are the portfolios with the smallest (top) and largest (bottom) integrals of the PSD with respect to frequencies from $3^{-1}\mathrm{h}^{-1}$ to $2^{-1}\mathrm{h}^{-1}$ out of all the possible combinations of seven wind farms. The 5th and 95th percentiles (PCTL) of the hourly step change function of the total wind power time series per installed power is given in the bottom right corner of each example.

The optimization algorithm is performed for two additional cases. Case II: excluding two distant site locations - located $\geq$25 km apart from the rest of the sites. Case III: setting upper and lower boundaries for installed wind power capacity at each site. Also here, the optimization has only a small influence on the hourly fluctuations compared to if the wind farm capacities at the pre-defined wind farm site locations were equally distributed over all wind farms. However, comparing case II to the first case, the 5th and 95th percentiles of the hourly step change function are increased by 7%. The increase is found to be more pronounced when the two distant sites are excluded compared to if any other two site locations were to be excluded instead, demonstrating the importance of the smoothing effect from distant sites.

As the Faroe Islands consists of a limited spatial area, surrounded by ocean, far from any other land, the spatial distribution of wind farms is limited. To examine the achievable smoothing effect, PSD are generated for up to 14 aggregated wind turbine

https://doi.org/10.5194/wes-2022-14
Preprint. Discussion started: 22 March 2022

eawe european academy of wind energy
Open Access WIND ENERGY SCIENCE DISCUSSIONS

Table 3. The range of the 5th (second column) and 95th (third column) percentiles (PCTL) of the hourly step change function of the lumped power output time series for all possible combinations of n wind farms (left column) per installed wind power capacity; the wind farm capacities are equally distributed over all considered sites. The 5th (fourth column) and 95th (fifth column) percentiles of the hourly step change function for the combinations with the smallest integral with respect to frequencies from 3^{-1}h^{-1} to 2^{-1}h^{-1}.

n	5th PCTL	95th PCTL	5th PCTL_{OPT}	95th PCTL_{OPT}
1	[-0.2013;-0.1659]	[0.1668;0.2089]	-0.1682	0.1671
2	[-0.1793;-0.1301]	[0.1288;0.1789]	-0.1339	0.1354
3	[-0.1475;-0.1174]	[0.1173;0.1488]	-0.1198	0.1255
4	[-0.1339;-0.1086]	[0.1091;0.1341]	-0.1097	0.1110
5	[-0.1251;-0.1017]	[0.1029;0.1248]	-0.1043	0.1052
6	[-0.1173;-0.0974]	[0.0986;0.1201]	-0.0975	0.0999
7	[-0.1118;-0.0941]	[0.0953;0.1134]	-0.0955	0.0963
8	[-0.1068;-0.0928]	[0.0939;0.1094]	-0.0950	0.0960
9	[-0.1030;-0.0917]	[0.0926;0.1050]	-0.0919	0.0938
10	[-0.1011;-0.0906]	[0.0919;0.1022]	-0.0924	0.0936
11	[-0.0985;-0.0902]	[0.0913;0.0995]	-0.0907	0.0923
12	[-0.0961;-0.0905]	[0.0908;0.0971]	-0.0911	0.0908
13	[-0.0937;-0.0900]	[0.0913;0.0940]	-0.0910	0.0913

time series. Results show less smoothing as more wind farms are integrated. The smoothing effect is most evident at the highest frequencies, but clear for periods up to 1-2 days. It is also seen that the high frequency fluctuations are highly dependent on which of the individual site locations are considered. Good wind farm combinations, in order to minimize the 2-3 hourly power output fluctuation, are wind farms that are located distant from each other, while poor wind farm combinations consist of clustered wind farms. When building wind farms in four out of the fourteen good wind farm areas, optimized wind farm positioning decreases the 5th and 95th percentiles of the hourly step change function by 15% compared to poor wind farm combinations.

This study accentuates the importance of choosing the best wind farm sites in order to naturally balance the wind power fluctuations. A feature that should be of interest to an operator, as a more smooth time series result in less operating effort of the power grid.

A suggestion for a future study is to include diverse wind turbine models in the analysis. Taller future wind turbines on the islands are planed. Another suggestion for a future study is to expand the current study to include higher temporal resolutions of the data sets.

https://doi.org/10.5194/wes-2022-14
Preprint. Discussion started: 22 March 2022

eawe european academy of wind energy
Open Access WIND ENERGY SCIENCE DISCUSSIONS

Appendix A: Filtering for aliasing effect

The WRF-generated wind speed data set used in this study display artificial high frequency fluctuations from aliasing effect (Poulsen et al., 2021). Thus, before usage, these time series must be corrected: For each WRF-generated wind speed time series, the power spectral density is generated and corrected for aliasing effect using the method given in Kirchner (2005), with the parameters $fc = 1$ and $f\_limit = \frac{1}{1\ \mathrm{day}}$, see Fig. A1. By reversing the corrected spectral calculations, preserving the phase of the Fourier transform of the original time series, a new de-aliased time series is generated. Finally, the average wind speed value of the original time series is added to the de-aliased time series. Figure A2 displays an example of a scatter-plot between the WRF-generated wind speed time series before and after de-aliasing of the time series.

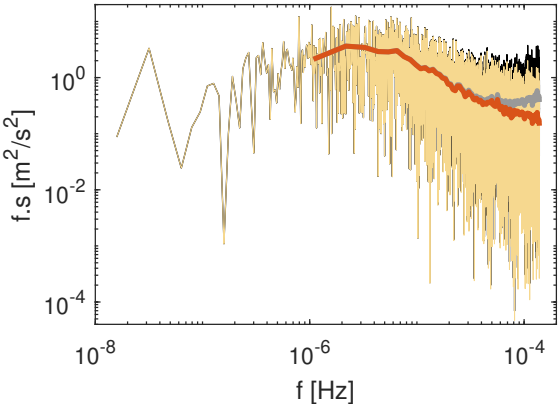

Figure A1. Black line represents raw PSD calculated from the WRF-generated wind speed time series at site C. Yellow superimposed line is the corresponding PSD corrected for aliasing effect using the method given in Kirchner (2005). Note that the black line is behind the yellow line. The gray and red lines represent the averaged PSD, from the black and yellow lines, respectively.

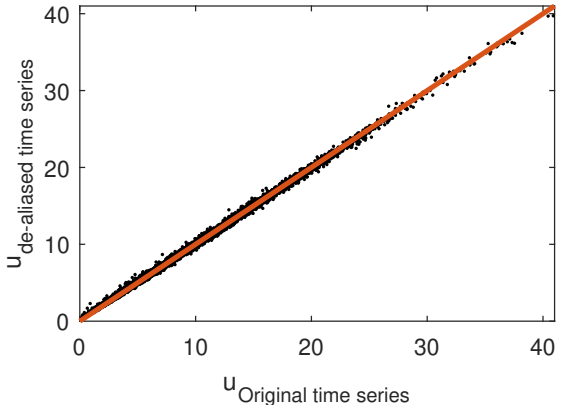

Figure A2. Scatter plot between WRF-generated wind speed time series at site C before (x-axis) and after (y-axis) de-aliasing of the time series.

https://doi.org/10.5194/wes-2022-14
Preprint. Discussion started: 22 March 2022

eawe european academy of wind energy
Open Access WIND ENERGY SCIENCE DISCUSSIONS

Author contributions. TP generated the results and wrote the initial manuscript. HGB supervised. All authors provided important input through discussion, feedback, and revision of the manuscript.

Competing interests. The authors declare that they have no conflict of interest.

Acknowledgements. The authors are grateful to the local power company SEV for giving access to measurements and WRF-generated data. We thank Kjeller Vindteknikk for their fast response to our questions regarding the WRF-generated data. TP acknowledges Equinor for their financial support of her Ph.D project "Analysis and modelling of the wind energy resources in the Faroe Islands".

https://doi.org/10.5194/wes-2022-14
Preprint. Discussion started: 22 March 2022

eawe european academy of wind energy
Open Access WIND ENERGY SCIENCE DISCUSSIONS

References

Barasa, M. and Aganda, A.: Wind power variability of selected sites in Kenya and the impact to system operating reserve, Renewable Energy, 85, 464 – 471, https://doi.org/https://doi.org/10.1016/j.renene.2015.05.042, 2016.

Beyer, H. G., Luther, J., and Steinberger-Willms, R.: Fluctuations in the combined power output from geographically distributed grid coupled wind energy conversion systems - an analysis in the frequency domain, Wind Engineering, 14, 179–192, 1990.

Beyer, H. G., Luther, J., and Steinberger-Willms, R.: Power fluctuations in spatially dispersed wind turbine systems, Solar Energy, 50, 297 – 305, https://doi.org/https://doi.org/10.1016/0038-092X(93)90025-J, 1993.

Cassola, F., Burlando, M., Antonelli, M., and Ratto, C. F.: Optimization of the Regional Spatial Distribution of Wind Power Plants to Minimize the Variability of Wind Energy Input into Power Supply Systems, Journal of Applied Meteorology and Climatology, 47, 3099 – 3116, https://doi.org/10.1175/2008JAMC1886.1, 2008.

Enercon: Enercon Product Overview, ENERCON GmbH, Aurich, Germany, April 2012, available at https://pdf.directindustry.com/pdf/enercon/enercon-product -overview/20877-243513.html, 2012.

Frank, C., Fiedler, S., and Crewell, S.: Balancing potential of natural variability and extremes in photovoltaic and wind energy production for European countries, Renewable Energy, 163, 674 – 684, https://doi.org/https://doi.org/10.1016/j.renene.2020.07.103, 2021.

Giebel, G.: Equalizing effects of the wind energy production in Northern Europe determined from reanalysis data, denmark. Forskningscenter Risoe. Risoe-R, No. 1182(EN), 2000.

Giebel, G.: On the benefits of distributed generation of wind energy in Europe, phD thesis from the Carl von Ossietzky Universität Oldenburg. Fortschr.-Ber. VDI Reihe 6 Nr. 444. Düsseldorf, VDI Verlag 2001. ISBN 3-18-344406-2, 2001.

Haslerud, A. S.: Faroe Islands - Detailed wind maps, Kjeller Vindteknikk, report number: KVT/ASH/2019/R032. Availability: limited to client, 2019.

Katzenstein, W., Fertig, E., and Apt, J.: The variability of interconnected wind plants, Energy Policy, 38, 4400 – 4410, https://doi.org/https://doi.org/10.1016/j.enpol.2010.03.069, 2010.

Kirchner, J. W.: Aliasing in $1f^{\alpha}$ noise spectra: Origins, consequences, and remedies, Phys. Rev. E, 71, 066 110, https://doi.org/10.1103/PhysRevE.71.066110, 2005.

Magnussen, J. P.: Vindmyllustaðseting - val av økjum til vindmyllulundir í Føroyum & dømi um staðsetingar, Orkudeildin á Umhvørvisstovuni, 2017.

Nanahara, T., Asari, M., Maejima, T., Sato, T., Yamaguchi, K., and Shibata, M.: Smoothing effects of distributed wind turbines. Part 2. Coherence among power output of distant wind turbines, Wind Energy, 7, 75–85, https://doi.org/https://doi.org/10.1002/we.108, 2004a.

Nanahara, T., Asari, M., Sato, T., Yamaguchi, K., Shibata, M., and Maejima, T.: Smoothing effects of distributed wind turbines. Part 1. Coherence and smoothing effects at a wind farm, Wind Energy, 7, 61–74, https://doi.org/https://doi.org/10.1002/we.109, 2004b.

Nørgaard, P. and Holttinen, H.: A Multi-Turbine Power Curve Approach, proceedings of Nordic Wind Power Conference, Gothenburg, 1-2 March 2004, pp. 1-5., 2004.

Palutikof, J., Cook, H., and Davies, T.: Effects of geographical dispersion on wind turbine performance in England: A simulation, Atmospheric Environment. Part A. General Topics, 24, 213–227, https://doi.org/https://doi.org/10.1016/0960-1686(90)90458-Y, 1990.

Pearre, N. S. and Swan, L. G.: Spatial and geographic heterogeneity of wind turbine farms for temporally decoupled power output, Energy, 145, 417 – 429, https://doi.org/https://doi.org/10.1016/j.energy.2018.01.019, 2018.

https://doi.org/10.5194/wes-2022-14
Preprint. Discussion started: 22 March 2022

Poulsen, T. and Beyer, H. G.: Spectral characteristics and spatial smoothing of wind power - a case study of the Faroe Islands, Meteorologische Zeitschrift, 29, 427–438, https://doi.org/10.1127/metz/2020/1041, 2020.

Poulsen, T., Niclasen, B., Giebel, G., and Beyer, H. G.: Validation of WRF generated wind field in complex terrain, Meteorologische Zeitschrift, 30, 413–428, https://doi.org/10.1127/metz/2021/1068, 2021.

Reichenberg, L., Johnsson, F., and Odenberger, M.: Dampening variations in wind power generation—the effect of optimizing geographic location of generating sites, Wind Energy, 17, 1631–1643, https://doi.org/https://doi.org/10.1002/we.1657, 2014.

Schlez, W. and Infield, D.: Horizontal, Two Point Coherence for Separations Greater Than the Measurement Height, Boundary-Layer Meteorology, 87, 459–480, https://doi.org/10.1023/A:1000997610233, 1998.

Sørensen, P., Cutululis, N. A., Vigueras-Rodríguez, A., Madsen, H., Pinson, P., Jensen, L. E., Hjerrild, J., and Donovan, M.: Modelling of power fluctuations from large offshore wind farms, Wind Energy, 11, 29–43, https://doi.org/https://doi.org/10.1002/we.246, 2008.

Tróndheim, H. M., Niclasen, B. A., Nielsen, T., Faria da Silva, F., and Bak, C. L.: 100% Sustainable Electricity in the Faroe Islands: Expansion Planning through Economic Optimisation, IEEE Open Access Journal of Power and Energy, 8, 23–34, https://doi.org/10.1109/OAJPE.2021.3051917, 2021.

Vigueras-Rodríguez, A., Sørensen, P., Viedma, A., Donovan, M., and Gómez Lázaro, E.: Spectral coherence model for power fluctuations in a wind farm, Journal of Wind Engineering and Industrial Aerodynamics, 102, 14 – 21, https://doi.org/https://doi.org/10.1016/j.jweia.2011.12.006, 2012.

Vincent, C., Larsén, X., Larsen, S., and Sørensen, P.: Cross-spectra over the sea from observations and mesoscale modelling, Boundary-Layer Meteorology, 146, 297–318, https://doi.org/10.1007/s10546-012-9754-1, 2013.

Wan, Y., Milligan, M., and Parsons, B.: Output Power Correlation Between Adjacent Wind Power Plants, Journal of Solar Energy Engineering, 125, 551–555, https://doi.org/10.1115/1.1626127, 2003.